5 Level Densities

Coordinator: A.V. Ignatyuk

Level densities represent one of key ingredients of nuclear reaction cross section calculations. Present Chapter, dealing with practical formalisms of nuclear level densities and their parameterization, is subdivided into three parts. First, the statistical model, notoriously used to calculate low energy nuclear reactions, needs detailed knowledge of total level densities and these are described in Section 5.1. Second, fission represents very specific reaction channel within the statistical model, and the corresponding fission level densities together with fission barriers are described separately in Section 5.2. Finally, extremely useful preequilibrium models of nuclear reactions require partial (particle-hole) level densities and these are described in Section 5.3.

5.1 Total Level Densities

Coordinator: A.V. Ignatyuk

Summary

For any applications of the statistical theory of nuclear reactions it is very important to obtain the parameters of the level density description from the reliable experimental data. The cumulative numbers of low-lying levels and the average spacings between neutron resonances are usually used as such data. The level density parameters fitted to such data are compiled in the RIPL Starter File for the tree models most frequently used in practical calculations:

i) For the Gilbert-Cameron model the parameters of the Beijing group, based on a rather recent compilations of the neutron resonance and low-lying level densities and included into the **beijing_gc.dat** file, are chosen as recommended. As alternative versions the parameters provided by other groups are given into the files: *jaeri_gc.dat*, *bombay_gc.dat*, *obninsk_gc.dat.* Additionally the *iljinov_gc.dat* and *mengoni_gc.dat* files include sets of the level density parameters that take into account the damping of shell effects at high energies.

ii) For the backed-shifted Fermi gas model the **beijing_bs.dat** file is selected as the recommended one. Alternative parameters of the Obninsk group are given in the *obninsk_bs.dat* file and those of Bombay in *bombay_bs.dat.*

iii) For the generalized superfluid model the Obninsk group parameters included into the **obninsk_bcs.dat** file are chosen as recommended ones and the *beijing_bcs.dat* file is included as an alternative set of parameters.

iv) For the microscopic approach to the level densities the files are: *obninsk_micro.for* — FORTRAN 77 source for the microscopical statistical level density code developed in Obninsk by Ignatyuk and coworkers, *moller_levels.gz* — Möller single-particle level and ground state deformation data base, *moller_levels.for* — retrieval code for Möller single-particle level scheme.

5.1.1 Introduction

The statistical properties of excited nuclear levels have been a matter of concern and study for over fifty years. One of the basic statistical properties of levels is their density. For the description of the level densities the Fermi-gas and constant temperature models are used frequently with parameters obtained from fitting some experimental data. But the physical assumptions upon which both these models are based are not sophisticated enough to allow them to account properly for variations of level densities over wide energy interval from the ground state to energies much higher than the neutron separation energy. This is not surprising, as the models discussed were initiated more than fifty years ago, when nuclear physics was in its infancy.

Some of the most important concepts, upon which current understanding of the structure of low-lying nuclear levels is based, include shell effects, pairing correlations and collective phenomena. All these concepts have been incorporated into the Generalized Superfluid Model (GSM) developed by many authors over the last 20 years. The phenomenological versions of the model convenient for an analysis of experimental data were developed intensively during the last years.

For practical applications of the statistical models it is very important to obtain parameters of the level density description from reliable experimental data. The cumulative numbers of low-lying levels and the average distances between neutron resonances are usually used as such data. The main problems of the corresponding parameter systematics are discussed briefly in this report. The systematics of the level density parameters developed during given RIPL project are considered below.

5.1.2 Composite Gilbert-Cameron Formula

Simple analytical expression expressions for the state density $\rho(U)$ of a nucleus with a given excitation energy U and the level density $\rho(U,J)$ of a nucleus with a given angular momentum J have been obtained by Bethe on the basis of the Fermi gas model [5.1]:

$$\begin{aligned} \rho(U) &= \frac{\sqrt{\pi}}{12a^{1/4}U^{5/4}}\exp(2\sqrt{aU}), \\ \rho(U,J) &= \frac{2J+1}{2\sqrt{2\pi}\sigma^3}\rho(U)\exp\left[-\frac{(J+1/2)^2}{2\sigma^2}\right]. \end{aligned} \tag{5.1}$$

Here $a=\pi^2 g/6$ is the level density parameter, which is proportional to the single-particle state density g near the Fermi energy, and σ^2 is the spin cutoff parameter.

For the Fermi gas model the state equations determining the dependence of the excitation energy U, the entropy S and other thermodynamic functions of a nucleus on its temperature t have a simple form:

$$U = at^2, \qquad S = 2at, \qquad \sigma^2 =< m^2 > gt, \tag{5.2}$$

where $< m^2 >$ is the mean square value of the angular momentum projections for the single-particle states around the Fermi energy, which may also be associated with the moment of inertia of a heated nucleus $\mathcal{I} = g < m^2 >$. The connection of thermodynamic functions (5.2) with the state and level densities (5.1) is obvious.

The main parameters of the Fermi-gas model may be estimated rather simply using the semi-classical approximation:

$$a = 2\left(\frac{\pi}{3}\right)^{4/3}\frac{m_0 r_0^2}{\hbar^2}A(1+\beta_s A^{-1/3}), \tag{5.3}$$

$$\mathcal{I}_0 = \frac{2}{5}\frac{m_0 r_0^2}{\hbar^2}A^{5/3}, \tag{5.4}$$

where m_0 is the nucleon mass, r_0 is the nuclear radius parameter, A is the mass number and β_s defines the surface component of the single-particle level density. Differences between various semi-classical determinations of the parameters (5.3) and (5.4) are mainly connected with large uncertainties of evaluation of β_s [5.2–5.5].

The most direct information on the level density of highly-excited nuclei is obtained from the average parameters of neutron resonances which were analyzed by many authors [5.6–5.15]. For the majority of nuclei the observed resonances correspond to s-neutrons, therefore the value of the average spacings D_0 is related to the level density of the compound nucleus by the relations:

$$D_0 = \begin{cases} \frac{1}{2}\left[\rho(B_n + \Delta E/2, I_0 + 1/2) + \rho(B_n + \Delta E/2, I_0 - 1/2)\right] & \text{for } I_0 \neq 0, \\ \frac{1}{2}\rho(B_n + \Delta E/2, 1/2) & \text{for } I_0 = 0, \end{cases} \tag{5.5}$$

were B_n is the neutron binding energy, ΔE is the energy interval for which the resonances are being examined, I_0 is the target nucleus spin, and the coefficient 1/2 before the sum takes into account the fact that s-neutrons form resonances only of a particular parity. If necessary, resonances for p-neutrons can be taken into consideration analogously.

The experimental values of D_0 are normally used as source data, from which the magnitude of the level density parameter can be derived by means of Eqs. (5.1) and (5.5). Many authors have carried out such an analysis [5.8, 5.10, 5.11]. The regular differences of the level densities for even-even, odd and odd-odd nuclei analogous to the even-odd differences of the nuclear masses have been already noted on the first systematics of experimental data. To take this effect into account it is usual to introduce the so-called effective excitation energy, defined as:

$$U^* = U - \begin{cases} \delta_Z + \delta_N & \text{for even} - \text{even} \\ \delta_Z & \text{for even } Z \\ \delta_N & \text{for even } N \\ 0 & \text{for odd} - \text{odd}, \end{cases} \tag{5.6}$$

where δ_I is the corresponding phenomenological correction for even-odd differences of the nuclear binding energies.

Data on the cumulative numbers of low-lying nuclear levels are also very important for the level density analysis. Many years ago it has been noted [5.8, 5.16] that the observed energy dependence of the cumulative number of levels is described rather well by the function

$$N(U) = \exp[(U - U_0)/T], \tag{5.7}$$

where U_0 and T are free parameters determined by the fitting to corresponding data. The quantity $N(U)$ is related to the level density by the relation

$$\rho_{lev}(U) = \frac{\mathrm{d}N}{\mathrm{d}U} = \frac{1}{T}\exp\left[(U - U_0)/T\right], \tag{5.8}$$

and it is obvious that the parameter T corresponds simply to a nuclear temperature. Since the value of this parameter is assumed to be constant over the energy range considered, Eq. (5.8) is called the constant temperature model.

In order to obtain a description of the level density for the whole range of excitation energies the low-energy dependence Eq. (5.8) should be combined with the high-energy dependence predicted by the Fermi-gas model. The link between both models' parameters can be found from the condition of continuity for the level density and its first derivative at some matching energy

$$U_x = U_0 + T \ln \rho_{fg}(U_x). \tag{5.9}$$

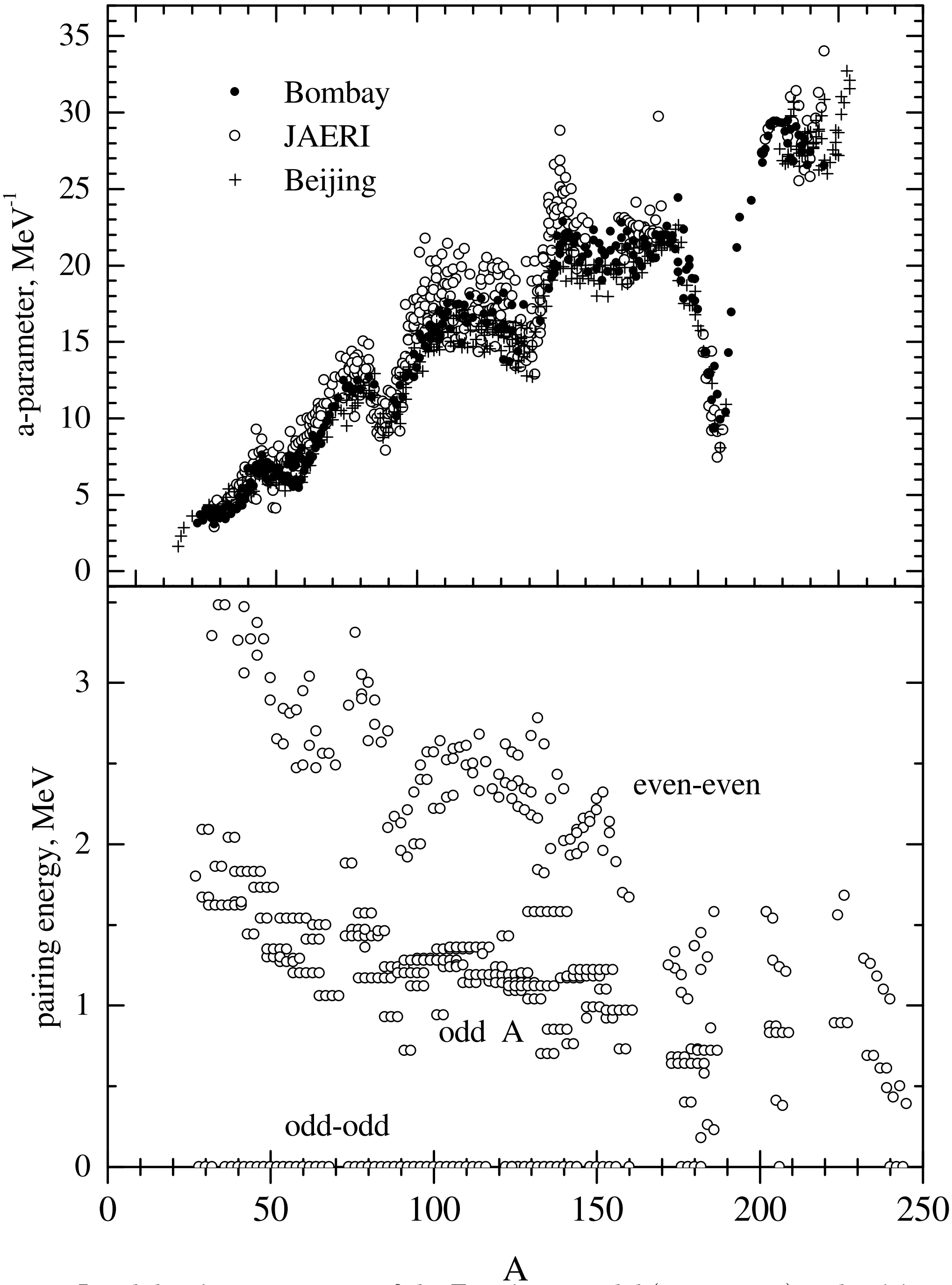

Figure 5.1: Level density parameters of the Fermi gas model (upper part) and pairing corrections to the nuclear binding energies (lower part).

The analysis of experimental data within the framework of this phenomenological approach has been carried out initially by Gilbert and Cameron [5.8], and the obtained parameters are shown in Figs. 5.1 and 5.2. The values of U_x determine the energies below which the level density description in terms of the Fermi-gas model becomes unsatisfactory, and one can see that for the majority of nuclei this energy is rather high.

Gilbert and Cameron [5.8] developed the systematics of the even-odd corrections to excitation

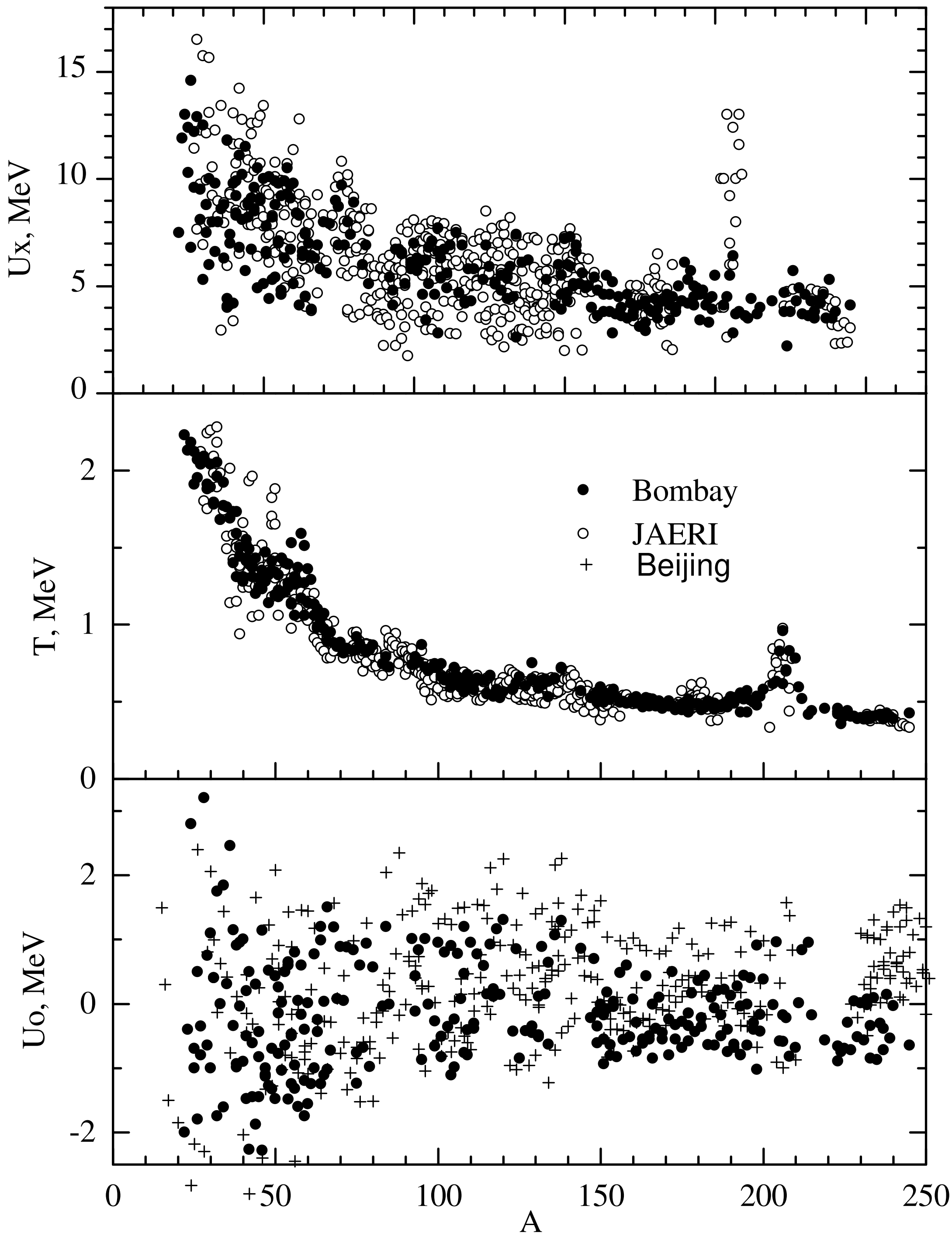

Figure 5.2: Level density parameters for the constant temperature model.

energies and suggested to approximate the shell changes of the level density parameters by the relation

$$\frac{a}{A} = 0.00917\,(S(Z) + S(N)) + Q(Z,N), \tag{5.10}$$

where $S(I)$ are the shell corrections for protons and neutrons, respectively, and $Q(Z,N) = 0.142$ for $54 < Z < 78$, $86 < N < 122$, and $Q(Z,N) = 0.120$ for $86 < Z < 122$, $130 < N < 182$. Such a definition of the level density parameters was combined with the analysis of experimental data on the cumulative numbers of low-lying levels, performed by the Bombay and JAERI groups, and the parameters obtained are shown in Figs. 5.1 and 5.2. Tables of parameters are included in the corresponding contribution files of the present CRP.

It should be pointed out that the values of the a- parameters obtained depend to some extent on the determination of the spin cutoff parameter. The primary systematics [5.8, 5.10] used the value of $< m^2 >= 0.146A^{2/3}$, which corresponds to mean-square averaging of the proton and neutron angular momentum projections over all single-particle levels occupied in the ground state of a nucleus. More correct values of $< m^2 >= 0.24A^{2/3}$ or directly the rigid body values of the moment of inertia were mostly used in following analyses. The differences in the choice of the spin cutoff parameters as well as some variations in the even-odd corrections of excitation energies should be borne in mind while comparing the a- parameters obtained by different authors.

Some adjusted versions of the tables for the shell and pairing corrections were proposed in Refs. [5.17, 5.18]. The systematics of the a-parameters differ from Eq. (5.10) only by the values of the numerical coefficients and a slightly different definition of the functions $Q(Z, N)$. The parameters of the Beijing group [5.18] are based on a rather recent compilations of the neutron resonance densities and numbers of low-lying levels, and after some corrections of contradictive data they are recommended as the most reliable for the including into the Starter File of the level density parameters.

One of the serious defects of all systematics considered so far is energy independence of the a-parameters. The results of all consistent microscopic calculations of the nuclear level densities display the damping of the shell effect at high excitation energies [5.19–5.21]. To include the shell effect damping into consideration the level density parameters should be energy dependent. This dependence may be approximated by the formula

$$a(U, Z, A) = \tilde{a}(A) \left\{ 1 + \frac{\delta E_0}{U} \left[1 - \exp(-\gamma U) \right] \right\}, \tag{5.11}$$

where $\tilde{a}$ is the asymptotic level density parameter to which $a(U)$ tends for high excitation energies, $\delta E_0 = S(N) + S(Z)$ is the shell correction energy[3] and γ is the damping parameter [5.22]. The shell corrections are determined

$$\delta E_0 = M_{exp}(Z, A) - M_{ld}(Z, A, \beta), \tag{5.12}$$

where M_{exp} is the experimental value of the mass defect and M_{ld} is the liquid drop component of the mass formula calculated for the equilibrium nuclear deformations β [5.23]. The analysis of the neutron resonance densities on the basis of Eqs. (5.11) and (5.12) was performed recently by Iljinov *et al.* [5.15] and Mengoni and Nakajima [5.24]. The parameters obtained are shown in the upper part of Fig. 5.3 in the form of the ratio a/A. The shell corrections used are displayed in the lower part of Fig. 5.3. These level density parameters are included into the Starter File as other versions of parameters of the Gilbert-Cameron formula and are recommended at excitation energies higher than 10 MeV.

Other systematics of the shell corrections must be studied to obtain more consistent description of the level density parameters at broad energy region.

[3]Microscopic energies defined in Chapter 1 represent the difference compared to the spherical macroscopic energy, and not the macroscopic energy at equilibrium nuclear deformation; their use for the shell corrections needed in the level density formulations is not fully appropriate.

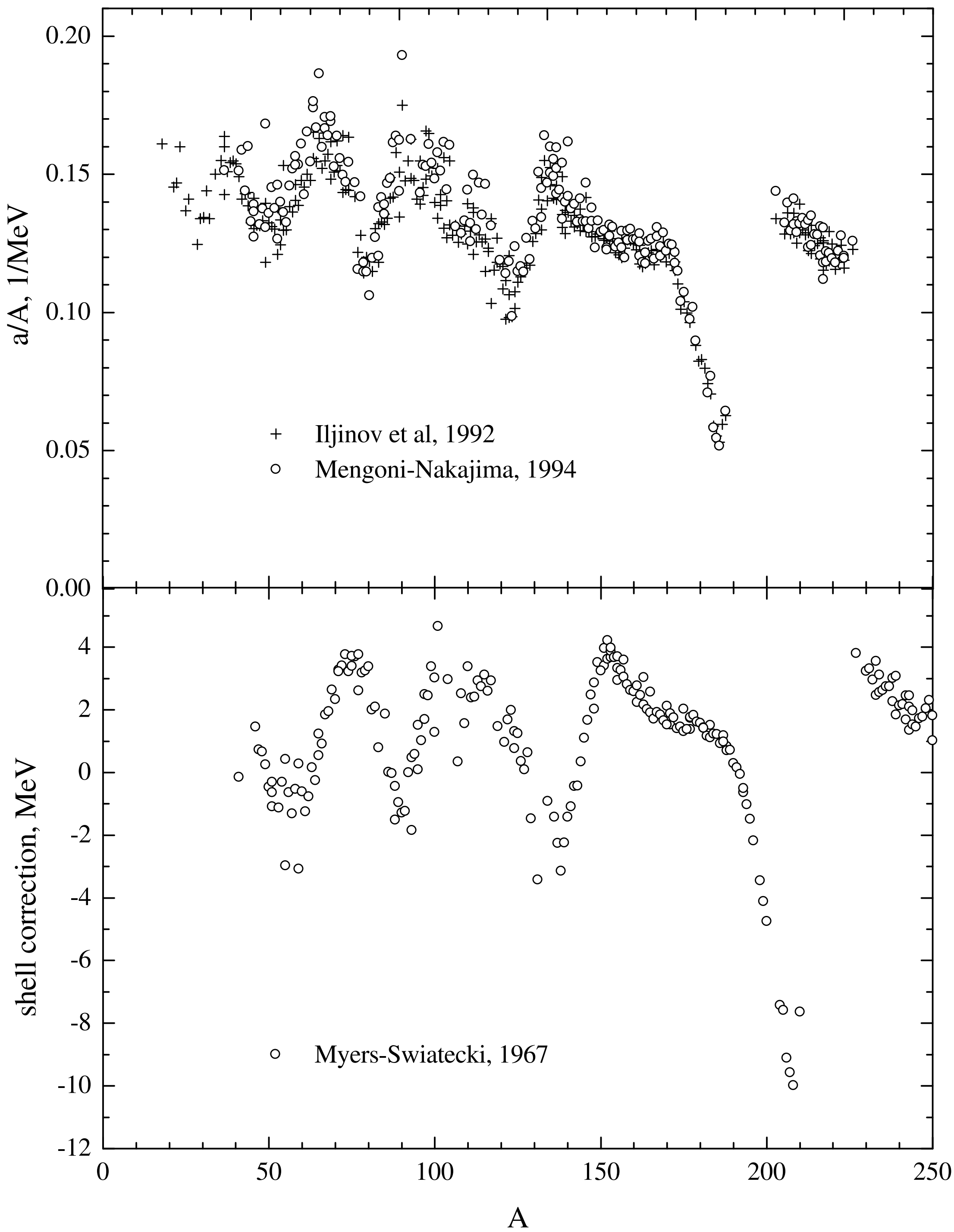

Figure 5.3: Ratio of the level density parameter a to the mass number A (upper part) and the shell corrections to the nuclear binding energies (lower part).

5.1.3 Back Shifted Fermi Gas Model

Another approach to the problem of simultaneous description of neutron resonance densities and low-lying levels was proposed in Ref. [5.12]. It has been assumed that both sets of experimental

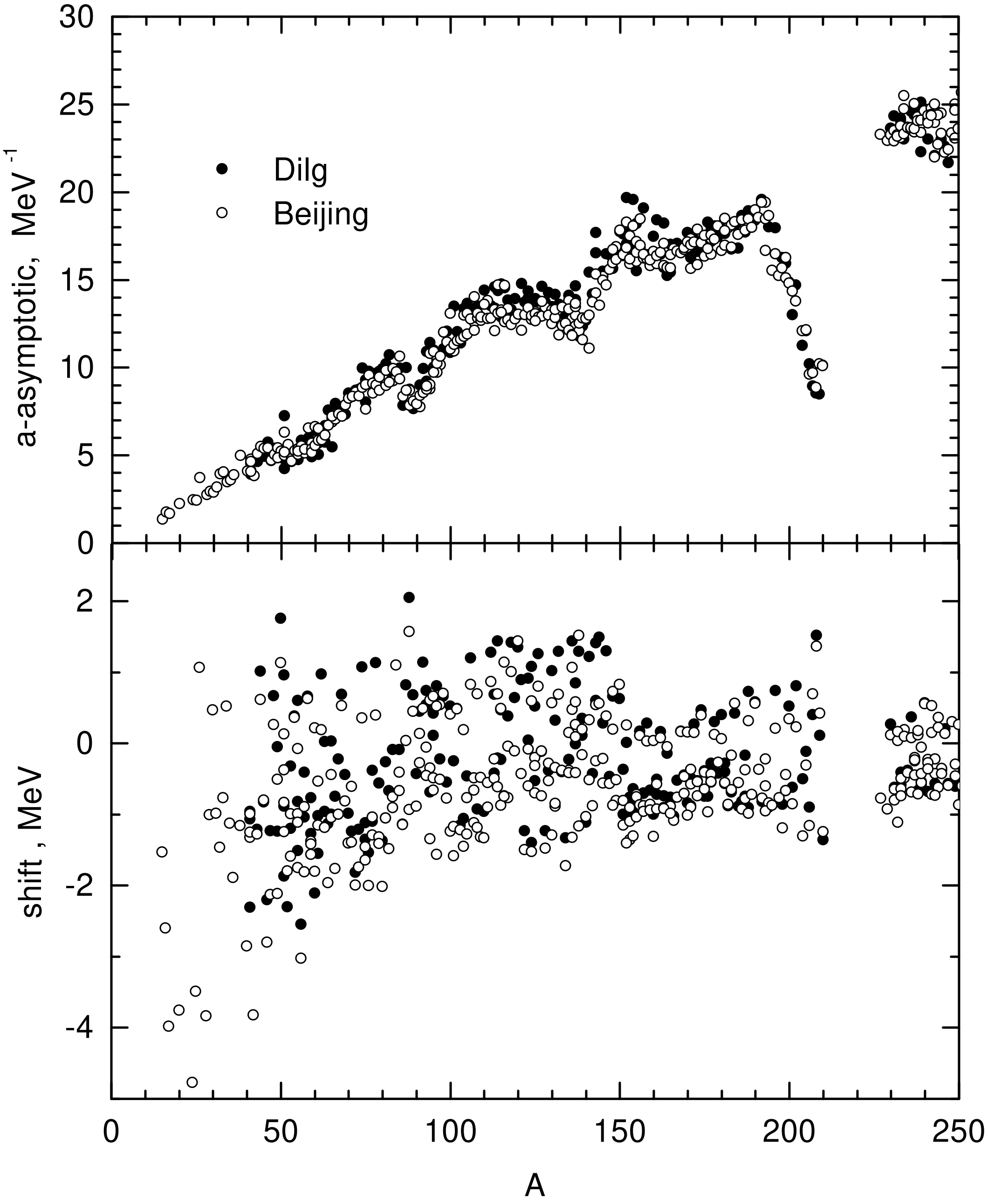

Figure 5.4: Level density parameters of the back-shifted Fermi gas model.

data can be described on the basis of the Fermi-gas relations if the level density parameter a and the excitation energy shift δ_{eff} are considered as free parameters for each nucleus. Since for odd-odd nuclei the displacement thus found is negative, the above approach has been called as the back-shifted Fermi-gas model. As the Fermi gas formulas are applied in this approach to a rather low excitation energies a more accurate estimation of a temperature is used

$$U - \delta_{eff} = at^2 - t. \tag{5.13}$$

U in denominator in the first line of Eq. (5.1) is to be replaced by $(U + t)$ [5.12].

Results of the corresponding analysis of the neutron resonance densities and low-lying nuclear levels are shown in Fig. 5.4. Due to another determination of effective excitation energies the values obtained for the a-parameter are naturally somewhat lower then those shown in Fig. 5.1. However, the shell effects in the mass dependence of a-parameters remain essentially invariable. The results of the recent analysis of more complete set of data performed by the Beijing group [5.25] are shown in Fig. 5.4 too. Difference between parameters obtained reflects improvements of experimental data achieved over recent years.

The spin cutoff parameters are determined in the model on the basis of the evaluation of the moment of inertia as the rigid body value or a half of this value. For many nuclei the available experimental data on the spins of low- lying levels can be used to analyze the statistical distribution of angular momentum. The distributions obtained agree rather with a half the rigid body values, but uncertainties of the spin-cutoff parameter estimations are still large for the final selection of the spin cutoff parameters.

Hence, both values for the moment of inertia are used in evaluation of the level density parameters. The parameters of Ref. [5.25] may be recommended as the Starter File for the back-shifted Fermi gas model. Again, as for the Gilbert-Cameron approach, it should be recommended to use Eq. (5.11) matched to these parameters to describe energy changes of the a-parameters above the neutron binding energies.

Up to now there is no a consistent systematics of parameters of the back-shifted Fermi gas model that could be used for parameter determination of nuclei for which there are no experimental data on the density of excited levels. Eq. (5.11) combined with the recent results of the low-lying nuclear level analysis [5.26] allow us to construct such a systematics, and this task can be recommended as the future stage of the RIPL development.

5.1.4 Generalized Superfluid Model

On the whole, all the results considered above let us to conclude that the Fermi-gas and constant temperature models provide us with comparatively simple and convenient formulas for parameterizing experimental data on nuclear level densities. However, these models do not give any explanation for the shifts of excitation energies and shell changes of the level density parameters. An interpretation of these effects must be obtained on the basis of more rigorous models that take into consideration shell inhomogenities of single-particle level spectra, on the one hand, and the superfluid and collective effects produced by the residual interaction of nucleons, on the other. A detailed discussion of such models can be found in the monograph [5.27]. However, rigorous microscopic methods of level density calculations are extremely laborious and this severely limits their application to experimental data analysis. For this reason there is a need for level density description, which takes into account the basic ideas of microscopic approaches concerning the structure of highly excited nuclear levels, while being sufficiently simple and convenient for broad application.

The influence of pairing correlations of super-conductive type on nuclear properties can be characterized by the value of the correlation functions $\Delta_{0\tau}$, which directly determine the even-odd differences in the nuclear binding energies and the energy gap $2\Delta_{0\tau}$ in the spectrum of quasi-particle excitations of even-even nuclei. The critical temperature t_c of the phase transition from a super-conductive (superfluid) state to normal one is also related to the correlation function:

$$t_c = 0.567\Delta_0. \tag{5.14}$$

The excitation energy corresponding to the critical temperature may be written as:

$$U_c = \frac{\pi^2}{6} g t_c^2 + \frac{1}{4} g \Delta_0^2 - n\Delta_0, \tag{5.15}$$

where $n = 0$, 1 and 2 for even-even, odd and odd-odd nuclei, respectively.

Above the critical energy the level density and other nuclear thermodynamic functions can be described by the Fermi gas relations in which the effective excitation energy is defined as

$$U^* = U - E_{cond}. \tag{5.16}$$

Here E_{cond} is the condensation energy that determines a reduction of the nuclear ground state energy due to the pairing correlations:

$$E_{cond} = \frac{1}{4} g \Delta_0^2 - n\Delta_0. \tag{5.17}$$

Below the phase transition point (5.14) the expressions for thermodynamic functions of a nucleus are rather complex, and they will not be considered here. Complete expressions can be found in Refs. [5.27–5.29].

If coherent collective effects are included into consideration of excited level structure, the nuclear level density may be expressed as

$$\rho(U) = \rho_{qp}(U) K_{vibr}(U) K_{rot}(U), \tag{5.18}$$

where ρ_{qp} is the level density due to quasi-particle excitations only, and K_{vibr} and K_{rot} are the corresponding enhancement coefficients due to vibration-al and rotational excitations, respectively.

In adiabatic approximation the rotational enhancement of the level density depends on the nuclear shape symmetry and can be written as [5.30]:

$$K_{rot} = \begin{cases} 1 & \text{for spherical nuclei,} \\ \mathcal{I}_\perp t & \text{for deformed nuclei,} \end{cases} \tag{5.19}$$

where $\mathcal{I}_\perp$ is the moment of inertia relatively to the perpendicular axis. This formula is obtained if the mirror and axial symmetry of deformed nuclei is assumed. The most stable nuclei of the rare- earth elements ($150 \leq A \leq 190$) and the actinide $A \geq 230$ have this shape. For non-axial forms the rotational enhancement of the level density becomes greater [5.30].

The vibrational enhancement coefficient is determined in the microscopic approach by the relation

$$K_{vibr} = \prod_i \left[\frac{1 - \exp(-\omega_i^0/t)}{1 - \exp(-\omega_i/t)} \right]^{g_i}, \tag{5.20}$$

where ω_i is the energy of vibrational excitations, ω_i^0 is the energy of corresponding quasi-particle excitation and g_i is the degeneracy of such excitations. The presence of quasi-particle energies in Eq. (5.20) reflects some account of non-adiabatic effects in excited nuclei. Due to symmetry conditions imposed on the nuclear Hamiltonian the rotational and vibrational excitations become connected in consistent microscopic approach [5.27]. As a result the calculated collective enhancement coefficients turn out always reduced in comparison to the adiabatic estimation.

It can readily be seen that adiabatic estimation of K_{rot} increases the nuclear level densities by a factor of 50–100 compared with the calculations based on quasi-particle excitations alone. The increase of the level density due to vibrational excitations will be appreciable only for low-energy excitations with $\omega_i < 1$–2 MeV.

During the last twenty years some microscopic models have been developed in order to consider collective effects in highly excited nuclei. The results of all these models demonstrate damping of level density enhancement factors with the increase of excitation energy. On the basis of the level density calculations within the SU-3 model (the oscillator mean field with the quadrupole-quadrupole interaction of particles) Hansen and Jensen [5.31] obtained the empirical function

$$K_{rot}(U) = \frac{K_{rot}^{adiab}(U)}{1 + \exp[(U - U_r)/d_r]}, \tag{5.21}$$

that describes damping of the rotational enhancement factors. The parameters of this formula were estimated as

$$U_r = 120A^{1/3}\beta^2\text{MeV}, \qquad d_r = 1400A^{-2/3}\beta^2\text{MeV}, \tag{5.22}$$

where β is the quadrupole deformation parameter. Some other phenomenological descriptions for the enhancement factor damping were discussed in Refs. [5.32–5.34]. All such descriptions include at least one or two parameters that can fluctuate from one nucleus to another. Up to now rather big uncertainty exists in estimation of the collective enhancement damping and unfortunately we have no reliable experimental data that could be used for a crucial test of available model predictions.

The vibrational enhancement of the level density was approximated by the relation

$$K_{vibr} = \exp[\delta S - (\delta U/t)], \tag{5.23}$$

where δS and δU are changes in the entropy and excitation energy, respectively, resulting from the vibrational modes. These changes are described by the relations of the Bose gas:

$$\begin{aligned} \delta S &= \sum_i (2\lambda_i + 1)[(1 + n_i)\ln(1 + n_i) - n_i \ln n_i] \\ \delta U &= \sum_i (2\lambda_i + 1)\omega_i n_i, \end{aligned} \tag{5.24}$$

where ω_i are the energies, λ_i the multi-polarities and n_i the occupation numbers for vibrational excitations at a given temperature. To account for the disappearance of collective enhancement of the level density at high temperatures, the occupation numbers were approximated by the relation

$$n_i = \frac{\exp(-\gamma_i/2\omega_i)}{\exp(\omega_i/t) - 1}, \tag{5.25}$$

where γ_i are the spreading widths of the vibrational excitations. The spreading of collective excitations in nuclei should be similar to the zero-sound damping in a Fermi liquid and the corresponding width can be written as

$$\gamma_i = C(\omega_i^2 + 4\pi^2 t^2). \tag{5.26}$$

The value of $C = 0.0075A^{1/3}$ MeV^{-1} was obtained from the systematics of the neutron resonance densities of medium-weight nuclei [5.35]. In that analysis, the experimental values were employed for the energies of the first 2^+ excitation and $\omega = 50A^{-2/3}$ MeV for the octupole excitations, whose influence, however, is much weaker than of the quadrupole ones.

The shell inhomogenities of the single-particle level spectra result in a particular energy dependence of the level density parameter $a(U)$. The shell effects on the level density become weaker with an increase of excitation energy, and at sufficiently high energies the dependence of parameter a on the mass number tends to the semi-classical value (5.3). These important features of the behavior of the level density parameters can be explained in the framework of the shell correction method [5.27]. The strong correlation of shell corrections (5.12) with the observed values of the ratios a/A (Fig. 5.3) can be used to construct a phenomenological systematics of the level density parameters [5.28]. The basis of the systematics is the relation, similar to (5.11),

$$a(U,Z,A) = \begin{cases} \tilde{a}(A)\left[1+\delta E_0 \frac{f(U^*)}{U^*}\right] & \text{for } U \geq U_c \\ a_c(U_c,Z,A) & \text{for } U < U_c, \end{cases} \tag{5.27}$$

where the function $f(U) = 1 - \exp(-\gamma U)$ determines the energy changes of the level density parameter at lower energies. The shell damping parameter $\gamma = 0.40A^{-1/3}$ MeV^{-1} was estimated on the basis of both the theoretical calculations and the analysis of experimental data [5.13, 5.28].

Applying Eqs. (5.14) to (5.17) to the description of pairing correlation effects the values of level density enhancement coefficients were estimated from the experimental data on the densities of neutron resonances. In such analysis the asymptotic values of the level density parameters were defined as $\tilde{a} = 0.073A + 0.115A^{2/3}$ MeV, the shell corrections were taken from Ref. [5.36] and the correlation functions were approximated by $\Delta_0 = 12/A^{1/2}$ MeV. The coefficients obtained are shown in the upper part of Fig. 5.5. In the lower part the values of similar coefficients calculated in the adiabatic approximation are given. A correlation of both coefficients is very strong but as a rule the adiabatic evaluations give higher values of coefficients than the ones extracted from the observed density of neutron resonances. The difference of these two definitions of the level density enhancement factors demonstrates that the damping of the enhancement coefficients for highly excited nuclei should be taken into account. For the global description of the nuclear level densities this damping may be taken into account by means of the empirical functions similar to (5.21) and (5.25).

To take into account possible shortcomings of the global systematics of the pairing correlation functions and collective enhancement damping an additional shift of the excitation energies

$$U_{eff} = U^* + \delta_{shift} \tag{5.28}$$

was introduced into Eq. (5.27) [5.35, 5.34]. Within the framework of such approach the set of parameters $\tilde{a}$ and δ_{shift} was obtained from the simultaneous fitting of the cumulative numbers of low-lying levels and observed neutron resonance densities recommended by this CRP [5.37]. The similar analysis was performed by the Beijing group at their compilation of the low-lying levels and neutron resonance densities [5.38]. The parameters obtained are shown in Fig. 5.6. The Obninsk group parameters are obtained on the basis of more recent compilation of the neutron resonance densities, and therefore these parameters are included as recommended in the RIPL Starter File.

For any practical application the individual parameters are preferable of course. Uncertainties of parameters are not very important for a prediction of the level densities in an intermediate energy region if experimental data for the neutron resonances and low-lying levels were chosen correctly. For the study of the nuclear level densities the analysis of evaporation spectra of different particles is of great interest. The energy dependencies of the level densities obtained from the spectrum analysis of various threshold reactions are in good agreement with the calculations based on the individual parameters of GSM [5.35].

On the other hand, for many tasks we need level density parameters for nuclei for which no experimental data is available. For such goals the global parameters may be used effectively. Also some local systematics of parameters may be proposed based on extrapolations of the isotopic or isotonic changes of the individual parameters. In many cases experimental data on the cumulative number of low-lying levels might be very useful because such data permit to fit one of the individual parameters keeping the global systematics for others.

At first glance it might seem that the systematics of the level density parameters in terms of the Fermi gas and the generalized superfluid model are equally justified, since they give

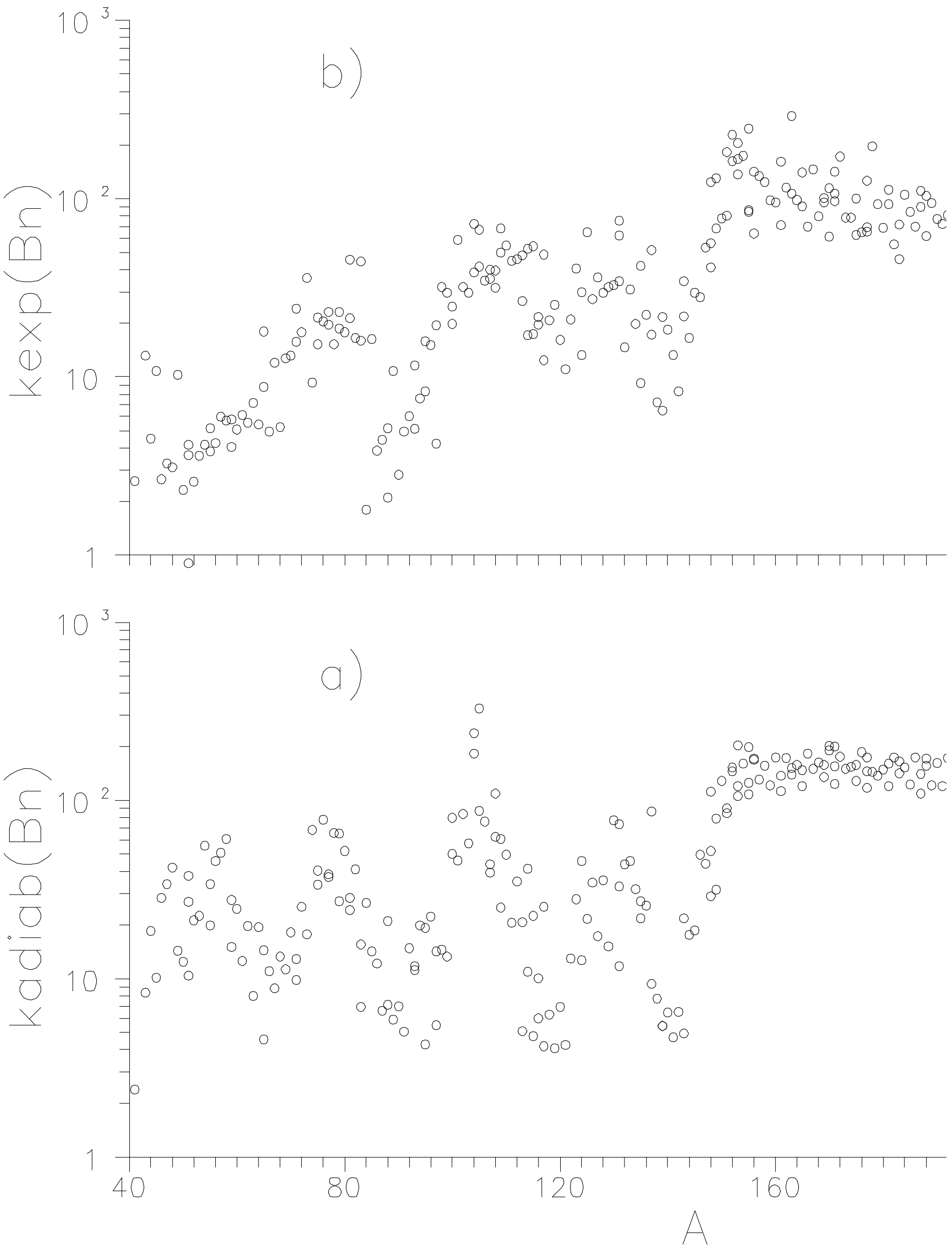

Figure 5.5: Collective enhancement factors calculated in the adiabatic approximation (a), and obtained as a ratio the observed density of neutron resonances to the calculated density of quasi-particle excitations (b).

approximately identical description of the level densities at excitation energies close to the neutron binding energy. However, these descriptions correspond to different absolute values of the level density parameters, because the inclusion of collective effects decreases the a-parameters obtained. These reduced values agree well enough with both the experimental data derived from the spectra of inelastically scattered neutrons with energies of up to 7 MeV and the theoretical calculations of the a-parameters for the single-particle level schemes of a Woods-Saxon potential [5.28]. This agreement of the data is very important, because the evaporation spectra are sensitive precisely to the value of the level density parameter. It is impossible to

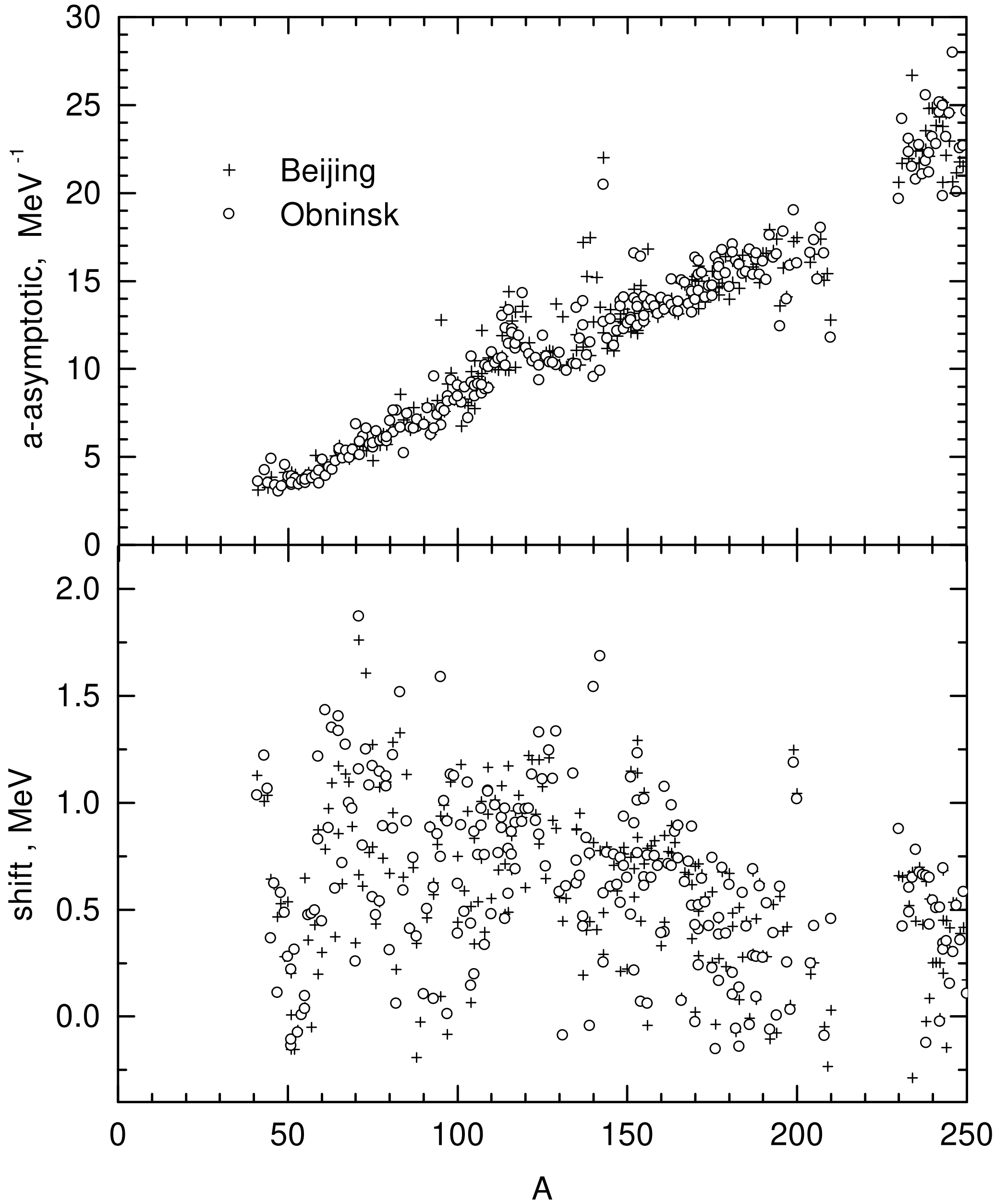

Figure 5.6: Level density parameters of the generalized superfluid model.

explain the differences between the values of a-parameter obtained from resonance data and from evaporation spectra in terms of the Fermi gas model without account of collective effects. Proper consideration of the level density collective enhancement is also very important for a consistent description of the observed fissilities of highly-excited nuclei [5.39].

Nowadays it seems almost obvious that in description of the level densities of excited nuclei we should use models which are more consistent than the Fermi-gas, but inevitably more complex. The success of the generalized superfluid model is attributed to the inclusion of the main well-known component of nuclear theory: the pairing correlations, shell effects and collective excitations. Some complexity of the model seems to be justified by the mutual consistency of the parameters obtained from the various experimental data and also by the close relation of the theoretical concepts used to describe the structure of low-lying nuclear levels and the statistical properties of highly excited nuclei.

5.1.5 Microscopic Generalized Superfluid Model

A more rigorous description of the level densities and other statistical characteristics of excited nuclei can be obtained in the framework of calculations performed with the realistic schemes of single-particle levels. The methods of such calculations are considered in details in the monograph [5.27]. The state equations for the thermodynamic functions of a excited nucleus, similar to Eq. (5.2) of the Fermi gas model, may be written in the form of

$$\begin{aligned} S &= \sum_i g_i[\beta E_i \overline{n}_i + \ln(1+\exp(-\beta E_i))], \\ U &= \frac{1}{2}\sum_i g_i[\sqrt{(\epsilon_i-\lambda)^2+\Delta_0^2} - E_i(1-2\overline{n}_i)] + \frac{\Delta_0^2-\Delta^2}{G}, \end{aligned} \tag{5.29}$$

Here $\beta = 1/t$ is the inverse temperature, E_i is the energy of quasiparticle nuclear excitations, $\overline{n}_i = [1+\exp(-\beta E_i)]^{-1}$ is the occupation numbers for the corresponding single-particle levels, g_i is the degeneracy of these levels and the sums over i include all single-particle levels for both protons and neutrons. The quasiparticle energies $E_i = [(\epsilon_i - \lambda_\tau)^2 + \Delta_\tau^2]^{1/2}$ are connected with the single-particle energies and the correlation function Δ_τ by the equations:

$$\begin{aligned} G_\tau^{-1} &= \frac{1}{4}\sum_i g_i \frac{1-2\overline{n}_i}{E_i}, \\ N_\tau &= \frac{1}{2}\sum_i g_i[1 - \frac{\epsilon_i-\lambda_\tau}{E_i}(1-2\overline{n}_i)], \end{aligned} \tag{5.30}$$

where N_τ is the number of protons or neutrons in a nucleus, λ_τ is the corresponding chemical potential and G_τ is the pairing force constant. For $t = 0$ Eqs. (5.30) determine the proton and neutron correlation functions for the ground state of a nucleus.

For given schemes of single-particle levels Eqs. (5.29) and (5.30) allow us to calculate the thermodynamic functions and the nuclear level densities without any additional parameter. To trace the difference between the behavior of the thermodynamic functions (5.29) and the Fermi gas ones (5.2), it is useful to determine the following functions:

$$\begin{aligned} a' &= S^2/4U, \qquad \overline{a} = \frac{\pi^2}{6}\beta\sum_i g_i\overline{n}_i(1-\overline{n}_i), \\ \overline{m^2} &= \frac{pi^2}{6\overline{a}}\beta\sum_i m_i^2 g_i \overline{n}_i(1-\overline{n}_i), \qquad \mathcal{I}_{\|} = \beta\sigma^2, \end{aligned} \tag{5.31}$$

which are equivalent to the Fermi gas model parameters. For low excitation energies the calculated values of the level density parameters (5.31) reproduce rather well the shell changes of the Fermi gas model parameters observed in experimental data (Figs. 5.1 and 5.4) [5.27]. At high excitation energies (> 50 MeV) the mass number dependence of calculated parameters is very close to the semiclassical (5.3).

The codes for microscopic calculations of the nuclear level densities are also given in the RIPL Starter File. The collective effects are included into the codes on the basis of the same approximations as for the phenomenological generalized superfluid model. As recommended ones for such calculations the single-particle level schemes of Möller *et al.* [5.40] are chosen. These schemes were used for calculations of the recommended nuclear binding energies, shell corrections and deformations (see Chapter 1). So their application to the level density calculations provides the consistency of the ground state and excited nucleus descriptions.

The single-particle level schemes and ground state deformations obtained in Ref. [5.40] are tabulated in the database *moller_levels.gz*. This set of single-particle level schemes was included in the RIPL in order to provide reliable and consistent single-particle level data set for microscopic nuclear level density calculations. The retrieval code *moller_levels.for* for the Möller data base is also provided. This is a modified version of the original code written by Nix [5.41]. It allows to extract interactively single particle level schemes for an given list of nuclides. The format of the output files is compatible with the microscopic nuclear level density codes *capote_micro.for* (Chapter 5.3) and *obninsk_micro.for* included in the RIPL Starter File.

5.1.6 Conclusions and Recommendations

Three level density models, the Gilbert-Cameron approach, the back-shifted Fermi gas model and the generalized superfluid model, are widely used in practical calculations of nuclear level densities. Therefore, recommended parameters for each level density model are presented in the RIPL Starter File.

The files of the level density parameters provided by the Beijing, Bologna, Bombay, JAERI and Obninsk groups were included into the Starter File as complete compilations of the level density parameters in computer readable format. Differencies among parameters obtained by different groups reflect different choices of input data on the neutron resonance spacings and on cumulative numbers of low-lying levels.

The following sets of parameters are included into the Starter File as recommended for each model:
i) For the Gilbert-Cameron model the parameters of the Beijing group [5.38], based on a recent compilation of the neutron resonance densities and numbers of low-lying levels, seem to be the best ones. The energy changes of these parameters at high excitation energies should be taken into account on the basis of formulae similar to Eq. (5.11). Such changes are particularly important for near magic nuclei. As an alternative version that includes more consistent description of shell effects at high energies, the parameters by Iljinov *et al.* [5.34] and Mengoni-Nakajima [5.24] could be used.
ii) For the back-shifted Fermi gas model, the parameters of Ref. [5.25] are included with two versions used for the moment of inertia. Again, as in the case of the Gilbert-Cameron approach, it is recommended to use Eq. (5.11) to describe energy changes of the a-parameter above neutron binding energy.
iii) For the generalized superfluid model, the Obninsk group parameters, obtained on the basis of more recent compilation of neutron resonance densities, are recommended.

A new analysis of available data on cumulative numbers of low-lying levels was performed within the frame of this CRP [5.26]. The nuclear temperatures and even-odd energy shifts are estimated now for a much larger number of nuclei than considered in previous analyses. Some more accurate evaluations of the neutron resonance densities are also obtained, and only a part of them taken into account by current systematics of the level density parameters. Re-evaluation of the level density parameters on the basis the new data obtained for the low-lying levels and neutron resonances is recommended for the next stage of the Starter File development. Other systematics of the shell corrections should be studied to obtain more consistent description of the level density parameters in broad energy region.

The use of microscopic methods is an alternative to semiempirical formulae for nuclear level density calculations. Combining microscopic and semimicroscopic methods, and using consistent set of single-particle levels, a deeper understanding of nuclear level densities can be achieved.

5.2 Fission Level Densities

Coordinator: V.M. Maslov

Summary

Fission level densities (or fissioning nucleus level densities at fission saddle deformations) are required for statistical model calculations of actinide fission cross sections. Back-shifted Fermi-Gas Model, Constant Temperature Model and Generalized Superfluid Model (GSM) are widely used for the description of level densities at stable deformations. These models provide approximately identical level density description at excitations close to the neutron binding energy. It is at low excitation energies that they are discrepant, while this energy region is crucial for fission cross section calculations. A drawback of back-shifted Fermi gas model and traditional constant temperature model approaches is that it is difficult to include in a consistent way pair correlations, collective effects and shell effects. Pair, shell and collective properties of nucleus do not reduce just to the renormalization of level density parameter a, but influence the energy dependence of level densities. These effects turn out to be important because they seem to depend upon deformation of either equilibrium or saddle-point. These effects are easily introduced within GSM approach [5.28]. Fission barriers are another key ingredients involved in the fission cross section calculations. Fission level density and barrier parameters are strongly interdependent. This is the reason for including fission barrier parameters along with the fission level densities in the Starter File.

The recommended file is **maslov.dat** — fission barrier parameters. Recent version of actinide fission barrier data obtained in Obninsk (*obninsk.dat*) should only be considered as a guide for selection of initial parameters. These data are included in the Starter File, together with the fission barrier parameters recommended by CNDC (*beijing.dat*), for completeness.

5.2.1 Introduction

Fission level densities and fission barrier parameters are key ingredients of actinide fission calculations. The important point is that fission level density and barrier parameters are strongly interdependent. The level density of deformed nucleus depends on the collective properties, pair correlations, and shell structure of a nucleus. These effects are easily introduced within the framework of the Generalized Superfluid Model [5.28]. Data on neutron-induced fission cross sections provide a sound basis for extraction of fission barrier parameters and for modeling level density approach. We proceed within the full-scale Hauser-Feshbach theory, coupled channel optical model and double-humped fission barrier model [5.42]. This approach is supported by many experimental signatures which demonstrate the importance of the collective, pairing, and shell effects both at equilibrium and saddle deformation.

Total nuclear level density is represented as a product of quasi-particle and collective contributions. The collective contribution to the level density at a saddle point is defined by the order of symmetry of a saddle point, which can be adopted according to the calculations within the shell correction method, such as the ones by Howard and Möller [5.43]. These saddle asymmetries depend on Z and N of the fissioning nucleus.

The effect of the pair correlations on the level density was demonstrated in the measurements of statistical $\gamma-$decay spectra on even rare-earth nuclei [5.44, 5.45]. In case of even-even fissioning nuclei step-like structure of the K_o^2 parameter, defining the angular anisotropy of fission fragments, is interpreted as being due to few-quasi-particle excitations. These excitations are essential for state density calculation at low intrinsic excitation energies. Contrary to the fission cross section, the structure observed in the behavior of the K_o^2 parameter, is virtually insensitive to the detailed shape of the fission level density. It was demonstrated that the observed irregularities in neutron-induced fission cross sections can be attributed to the interplay of few-quasi-particle excitations in the level density of fissioning and residual nuclei [5.46, 5.47].

The shell structure effects are introduced through the dependence of the level density $a-$parameter on the excitation energy. Damping of the shell effects influences the shape of first-chance fission cross section at excitation energies above fission threshold. The impact of pairing correlations and of collective and shell effects, on the calculated fission cross sections depends on the excitation energy [5.48, 5.49].

It was demonstrated that the sophisticated level density approach, involving pair, shell and collective effects, is unavoidable.

5.2.2 Fission Level Densities

In the adiabatic approximation the total nuclear level density $\rho(U, J, \pi)$ is represented as a product of quasi-particle and collective contributions,

$$\rho(U, J, \pi) = K_{rot}(U, J) K_{vib}(U) \rho_{qp}(U, J, \pi), \tag{5.32}$$

where $\rho_{qp}(U, J, \pi)$ is the quasi-particle level density, and $K_{rot}(U, J)$ and $K_{vib}(U)$ are rotational and vibrational enhancement factors. The collective contribution to the level density of a deformed nucleus is defined by the symmetry order of nuclear deformation. The actinide nuclei equilibrium deformation is axially symmetric. The symmetry order of nuclear shape at inner and outer saddle point is adopted according to the calculations performed using shell correction method [5.43].

Level densities at equilibrium deformations should reproduce both: (i) the average neutron resonance spacings and (ii) the observed cumulative number of discrete levels $N^{exp}(U)$ (see previous Chapter). In the latter case, GSM model fails to describe the cumulative number of low-lying levels without introduction of the additional shift in the excitation energy δ_{shift}. Therefore, level densities at low excitation energies (i.e. just above the last discrete level where $N^{exp}(U) \sim N^{theor}(U)$) a modified constant temperature model is applied. The constant temperature approximation

$$\rho(U) = dN(U)/dU = T^{-1} \exp((U - U_o)/T), \tag{5.33}$$

is extrapolated up to the matching point U_c above which the GSM model [5.28] is adopted. The following condition is imposed:

$$U_c = U_o - T \ln(T \rho(U_c)). \tag{5.34}$$

Here, the odd-even energy shift $U_o = -n\triangle$, where $\triangle = 12/\sqrt{A}$ is the pairing correlation function, A is a mass number, and $n = 0$ for even-even, 1 for odd and 2 for odd-odd nuclei. The value of nuclear temperature T is defined by the matching conditions at excitation energy U_c. The constant temperature model parameters for some actinides are given in Table 5.1.

The respective parameters for axially symmetric fissioning nucleus (nuclear temperature T_f and excitation energy shift U_{of}) are defined at the matching energy U_{cf}, which is assumed to be the same as for the equilibrium deformation (U_c). This is a fair approximation because for ground state deformations the U_c value is not very much sensitive to the value of the $a-$parameter. The

Table 5.1: Constant temperature model parameters.

Parameter	^{246}Cm	^{245}Cm	^{241}Am	^{242}Am
U_c, MeV	3.6	2.4	3.6	2.4
U_o, MeV	-0.0068	-0.65311	-0.96455	-1.6452
T, MeV	0.37326	0.36246	0.40723	0.39241

effects of non-axiality and mass asymmetry are included afterwards. At excitation energies above U_{cf} the GSM model [5.28] is applied.

The parameters of the level density model for the inner (outer) saddle points and equilibrium deformations are:

- main level density parameters a_f and a,
- shell corrections $\delta W_{fA(B)}$ and δW,
- pairing correlation functions Δ_f and Δ , at equilibrium deformations Δ_o =$12/\sqrt{A}$,
- quadrupole deformation ε,
- moment of inertia at zero temperature $\mathcal{I}_0/\hbar^2$

Values of these parameters for actinides are given in Table 5.2. Shell corrections for ground state deformations are calculated as $\delta W = M^{exp} - M^{MS}$, where M^{MS} denotes liquid drop mass (LDM), calculated with Myers-Swiatecki parameters [5.23], and M^{exp} is the experimental nuclear mass. Shell correction values at inner and outer saddle deformations $\delta W_{fA(B)}$ are taken from the comprehensive review by Bjornholm and Lynn [5.50]. Correlation function Δ_f =$\Delta_o + \delta$ at saddle-point depends on a_f/a ratio, which is a function of $(\delta W_f - \delta W)$.

Table 5.2: Level density parameters for fission and neutron emission channels in actinide nuclei.

Parameter	inner saddle (A)	outer saddle (B)	neutron channel
δW, MeV	2.5**	0.6	LDM
Δ, MeV	Δ_o $+\delta$ *	Δ_o $+\delta$ *	Δ_o
ε	0.6	0.8	0.24
$\mathcal{I}_0/\hbar^2$, MeV^{-1}	100	200	73

**) for axially asymmetric deformations, 1.5 MeV for axially symmetric deformations;
*) $\delta = \Delta_f - \Delta$ value is defined by fitting fission cross section in the plateau region.

Values of the $\tilde{a}-$parameter are determined by fitting neutron resonance spacings $\langle D_{obs}\rangle$. These, along with the $s-$wave neutron strength function $\langle S_o\rangle$, are obtained taking into account the correction for resonances missing due to their weakness and/or to poor experimental resolution [5.51]. Essentially, these values are consistent with those recommended for the RIPL Starter File (see file *obninsk.dat*). The shell correction dependence of $a-$parameter is defined using the following equation [5.28]:

$$a(U) = \begin{cases} \tilde{a}(1+\ \delta W f(U-E_{cond})/(U-E_{cond})), & U > U_{cr} = 0.47 a_{cr}\Delta^2\ - n\Delta \\ a(U_{cr}) = a_{cr} & U \le U_{cr} = 0.47 a_{cr}\Delta^2\ - n\Delta, \end{cases} \tag{5.35}$$

where $n = 0$, 1, 2 for even-even, odd-A and odd-odd nuclei, respectively; $f(x) = 1 - \exp(-\gamma x)$ is the dimensionless function describing damping of the shell effects; condensation energy $E_{cond} =$

$0.152 a_{cr} \Delta^2$, where Δ is the correlation function; $\tilde{a}$ is the asymptotic a-parameter value at high excitation energies. It is assumed that $\tilde{a}$-values for equilibrium and saddle deformations are identical.

This means that the complete expression for the constant temperature approach to the total level density reads

$$\rho(U) = K_{rot}(U) K_{vib}(U) \frac{\omega_{qp}(U)}{\sqrt{2\pi}\sigma} = T^{-1} \exp((U - U_o)/T). \tag{5.36}$$

The quasi-particle state densities $\omega_{qp}(U)$ are renormalized at excitation energies $U < U_c$. Here, $\sigma^2 = \mathcal{I}_{\|}\ t$ is the spin distribution parameter, t is thermodynamic temperature, the parallel moment of inertia $\mathcal{I}_{\|} = 6/\pi^2 < m^2 > (1 - 2/3\varepsilon)$, where $< m^2 >$ is the average value of the squared projection of the angular momentum of the single-particle states, and ε is quadrupole deformation parameter.

For deformed axially symmetric nucleus it is assumed

$$K_{rot}(U) = \sigma_\perp^2 = \mathcal{I}_\perp t = 0.4 m r_o^2 \hbar^{-2} (1 + 1/3\varepsilon), \tag{5.37}$$

where $\sigma_\perp^2$ is the spin cutoff parameter, $\mathcal{I}_\perp$ is the nuclear moment of inertia (perpendicular to the symmetry axis). $\mathcal{I}_\perp$ is taken equal to the rigid-body value at high excitation energies (at which pairing correlations are destroyed), while experimental value is adopted at zero temperature. In the intermediate range, values interpolated using the GSM equations [5.28] are used.

For $\gamma-$asymmetric nuclides the rotational enhancement factor is

$$K_{rot}(U) = 2\sqrt{2\pi}\sigma_\perp^2 \sigma. \tag{5.38}$$

The closed-form expressions for the thermodynamic temperature and other relevant equations needed to calculate $\rho(U, J, \pi)$ are provided by the GSM model [5.28]. Mass asymmetry increases level densities by a factor of 2.

The quasi-particle level density $\rho_{qp}(U, J, \pi)$ is defined as

$$\rho_{qp}(U, J, \pi) = \frac{(2J+1)\omega_{qp}(U)}{4\sqrt{2\pi}\sigma_\perp^2 \sigma} \exp\left(-\frac{J(J+1)}{2\sigma_\perp^2}\right). \tag{5.39}$$

Few-quasi-particle effects, due to pairing correlations, are essential for state density calculation at low intrinsic excitation energies of recently. The section was shown to two-quasi-particle configurations ^{238}Pu [5.52]. The same effect is observed in the ^{238} U(n,γ) data due to (n,γ n') reaction competition [5.53]. It was demonstrated that effects are important for reproducing fission cross sections below ~2 MeV incident neutron energy [5.46, 5.54]. Observed irregularities in neutron-induced fission cross be attributed to the interplay of few-quasiparticle the level density of fissioning and residual nuclei. $n-$quasiparticle state densities, which sum-up to the intrinsic state density of quasiparticle excitations can be estimated using Bose-gas model predictions [5.52, 5.55]

$$\omega_{qp}(U) = \sum_n \omega_{nqp}(U) = \sum_n \frac{g^n (U - U_n)^{n-1}}{((n/2)!)^2 (n-1)!}, \tag{5.40}$$

where $g = 6a_{cr}/\pi^2$ is a single-particle state density at the Fermi surface, and n is the number of quasi-particles. This equation provides energies. Partial state densities $\omega_{nqp}(U)$ depend critically on the excitation of the n-quasi-particle odd-A nuclei, n = 2, 4, ... for even-even and odd-odd nuclei). The discrete character of few-quasi-particle excitations is unimportant only in the case of odd-odd nuclei. The values of U_n are given by [5.55]

$$U_n = \begin{cases} E_{cond}(3.23n/n_{cr} - 1.57n^2/n_{cr}^2), & \text{if } n < 0.446\ n_{cr} \\ E_{cond}(1 + 0.627n^2/n_{cr}^2), & \text{if } n \geq 0.446\ n_{cr}. \end{cases} \tag{5.41}$$

Here, $n_{cr} = 12/\pi^2(\ln 2)gt_{cr}$, $t_{cr} = 0.571\Delta$ is a critical temperature, and $E_{cond} = 0.152a_{cr}\Delta^2 - m\Delta$ is a condensation energy (with m=0, 1, 2 for even-even, odd-A and odd-odd nuclides, respectively). Eq.5.41 takes into account the energy dependence of the correlation function $\Delta(U)$ and a modified Pauli correction to the excitation energy. The angular momentum distribution parameter σ^2 can be written as

$$\sigma^2 = \sum_n n\langle m^2\rangle\omega_{nqp}(U)/\sum_n \omega_{nqp}(U), \tag{5.42}$$

where $\langle m^2\rangle = 0.24A^{2/3}$ is the average value of the squared projection of the angular momentum of the single-particle states on the symmetry axis.

The pairing is weakened by excitation of few-quasi-particle states. Actually, only the lowest-number quasi-particle states (n =2 for even nuclei and n =1 for odd nuclei) lead to the pronounced structure in the total level density for actinide nuclei [5.52]. In the case of even-even nuclei, at excitations below four-quasi-particle excitation threshold, the intrinsic state density $\omega_2(U)$ can be represented by Eq. (5.40) modified with a Woods-Saxon type factor:

$$\omega_2(U) = g^2(U_4 - U_2 - \alpha)\left[1 + \exp((U_2 - U + \beta)/\gamma)\right]^{-1}. \tag{5.43}$$

This estimate of $\omega_2(U)$ was obtained by modeling the structure of ^{238}Pu intrinsic state density in order to interpret observed step-like structure in the ^{239}Pu(n,2n) reaction near the threshold [5.52].

To avoid the use Bose-gas equations (Eq. (5.40)) for the intrinsic state densities, the step-like behavior can be simulated within the constant temperature model. At excitation energies above the pairing gap (i.e. $U > U_2$) but below the four-quasi-particle excitation threshold, the level density $\rho(U)$ of an axially symmetric fissioning nucleus is calculated as

$$\rho(U) = \rho(U_4 - \delta_4)/(1 + \exp(U_2 - U + \delta_a)/\delta_s). \tag{5.44}$$

This estimate almost coincides with the predictions of the Bose-gas model. The numerical values: δ_4 =0.5 MeV, $\delta_a = 0.1 \div 0.2$ MeV, $\delta_s = 0.1 \div 0.2$ MeV were extracted by fitting fission cross section data. Fission level density for even-even nuclide ^{234}U at outer saddle, as calculated within the current approach (Eq. (5.44)), are compared with the constant temperature model approximation on Fig. 5.7. Collective levels are used below the threshold for the 2-quasi-particle excitations (U_2). In case of axial symmetry at the inner saddle the band-heads spectra are similar to that at equilibrium deformation. In case of axial asymmetry at the inner saddle the 2^+ band-heads are sufficiently lowered. The position of negative parity band $K^\pi = 0^-$ at outer saddle is lowered due to mass asymmetry (see Table 5.3)

In the case of odd-even and even-odd nuclei the partial contributions $\omega_{nqp}(U)$ of $n-$quasiparticle states to the total intrinsic state density $\omega_{qp}(U)$ produce a distinct "jump" only below the 3-quasi-particle excitation threshold (U_3). The level density of the fissioning nucleus at excitations $U > U_3$ may be calculated introducing odd-even excitation energy shift: $\hat{U} = U + \Delta_f$, where Δ_f is the correlation function for the saddle point deformation. Nuclear level density $\rho(U)$ up to the 3-quasi-particle excitation threshold U_3 is actually independent on the excitation energy, since the intrinsic state density ($\omega_1 \sim g$) is constant. Therefore, level densities in this energy region can be written as

$$\rho(U) = T_f^{-1}\exp((U_3 + \Delta_f - U_o - \delta_3)/T_f) \sim \exp((\Delta_f - U_o)/T_f). \tag{5.45}$$

Table 5.3: Transition spectra band-heads of even-even nuclei.

inner saddle			outer saddle	
K^π	$E^{ax}_{K^\pi}$, MeV	$E^{nonax}_{K^\pi}$, MeV	K^π	E_{K^π}, MeV
0^+	0.0	0.0	0^+	0.0
2^+	0.5	0.1	2^+	0.5
0^-	0.4	0.4	0^-	0.2
1^-	0.4	0.4	1^-	0.5
2^+	0.5	0.5	2^+	
2^-	0.4	0.4	2^-	
0^+	0.8	0.8	0^+	
0^+	0.8	0.8	0^+	

Table 5.4: Transition spectra band-heads of Z-odd, N-even nuclei.

inner saddle		outer saddle	
K^π	E_{K^π}, MeV	K^π	E_{K^π}, MeV
$3/2^-$	0.0	$5/2^+$	0.0
$5/2^+$	0.140	$5/2^-$	0.0
$7/2^-$	0.180	$3/2^+$	0.08
$5/2^-$	0.180	$3/2^-$	0.08
		$1/2^+$	0.04
		$1/2^-$	0.04
		$1/2^+$	0.05
		$1/2^-$	0.05

Above the 3-quasi-particle states excitation threshold the constant temperature model is used. However, for the excitation energies between 3-quasi-particle and 5-quasi-particle excitation thresholds, the level density can be slightly increased, as compared with the constant temperature approximation:

$$\rho(U) = T_f^{-1}\exp((U - U_o + \delta_5)/T_f). \tag{5.46}$$

The discrete transition state spectra, for excitation energies up to 200 keV, can be constructed using one-quasi-particle states by Bolsterli *et al.* [5.56]. Each one-quasi-particle state in odd fissioning nucleus is assumed to have a rotational band built on it with a rotational constant, depending on the respective saddle-point deformation (see Tables 5.4i and 5.5). Due to the axial asymmetry at the inner saddle we additionally assume $(2J+1)$ rotational levels for each J value. The positive parity bands $K^\pi = 1/2^+,\ 3/2^+,\ 5/2^+, \ldots$ at outer saddle are assumed to be doubly degenerated due to mass asymmetry [5.43]. The intrinsic 2-quasi-particle spectrum

Table 5.5: Transition spectra band-heads Z-even, N-odd nuclei.

inner saddle		outer saddle	
K^π	E_{K^π}, MeV	K^π	E_{K^π}, MeV
$1/2^+$	0.0	$1/2^+$	0.0
$5/2^+$	0.08	$1/2^-$	0.0
$1/2^-$	0.05	$3/2^+$	0.08
$3/2^-$	0.0	$3/2^-$	0.08
		$5/2^+$	0.0
		$5/2^-$	0.0

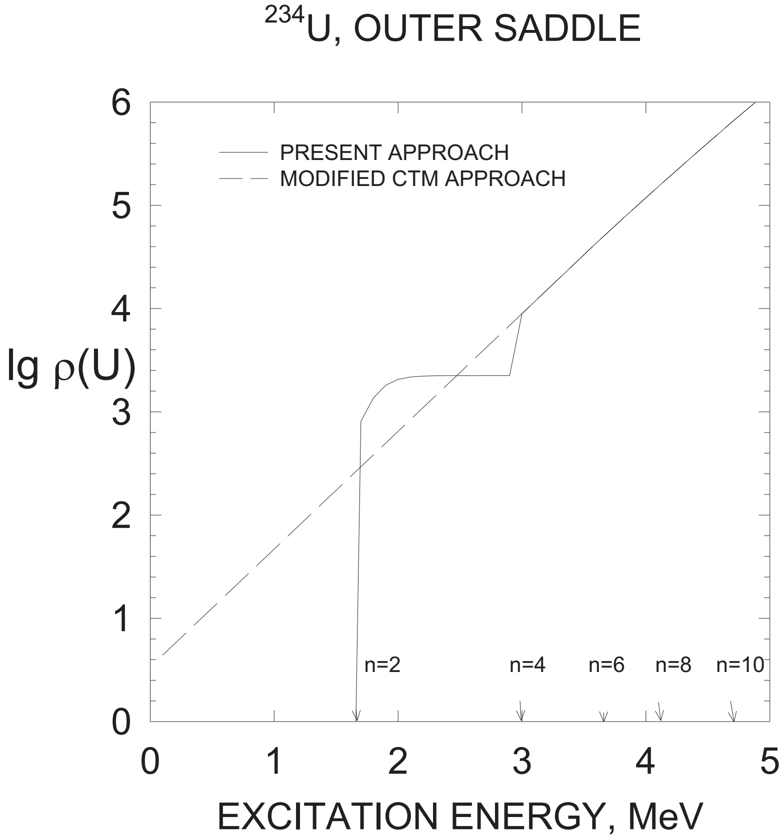

Figure 5.7: Level densities at outer saddle-point in ^{234}U. The arrows on the horizontal axis indicate excitation thresholds of even $n-$quasi-particle configurations.

of odd-odd nuclide ^{242}Am at equilibrium deformation can be obtained following Sood and Singh [5.57]. The expected location of still unobserved two-quasi-particle states was predicted (see Table 5.6). Using these intrinsic states as the band-head energies the rotational bands can be built in the same way as for Z-odd, N-even nuclei.

Table 5.6: Transition spectra band-heads of $Z-$odd, $N-$odd nuclei.

inner saddle		outer saddle	
K^π	E_{K^π}, MeV	K^π	E_{K^π}, MeV
1^-	0.0	1^-	0.0
0^-	0.044	0^-	0.044
5^-	0.049	5^-	0.049
6^-	0.170	6^-	0.170
1^-	0.220	1^-	0.220
3^-	0.242	$3-$	0.242
2^-	0.288	2^-	0.288

The values of δ_3 and δ_5 parameters can be defined by fitting fission cross section data. The level densities calculated with Eqs. (5.45) and (5.46) at the inner saddle-point of ^{239}Pu are shown on Fig. 5.8.

Adopting fission and total level densities modeling described above fission barrier parameters were extracted from the experimental neutron-induced fission cross sections on $^{232-238}$U, $^{238-244}$Pu, $^{241-243}$Am, and $^{242-248}$Cm targets [5.58–5.63]. Fission barrier parameters for Th, Pa,

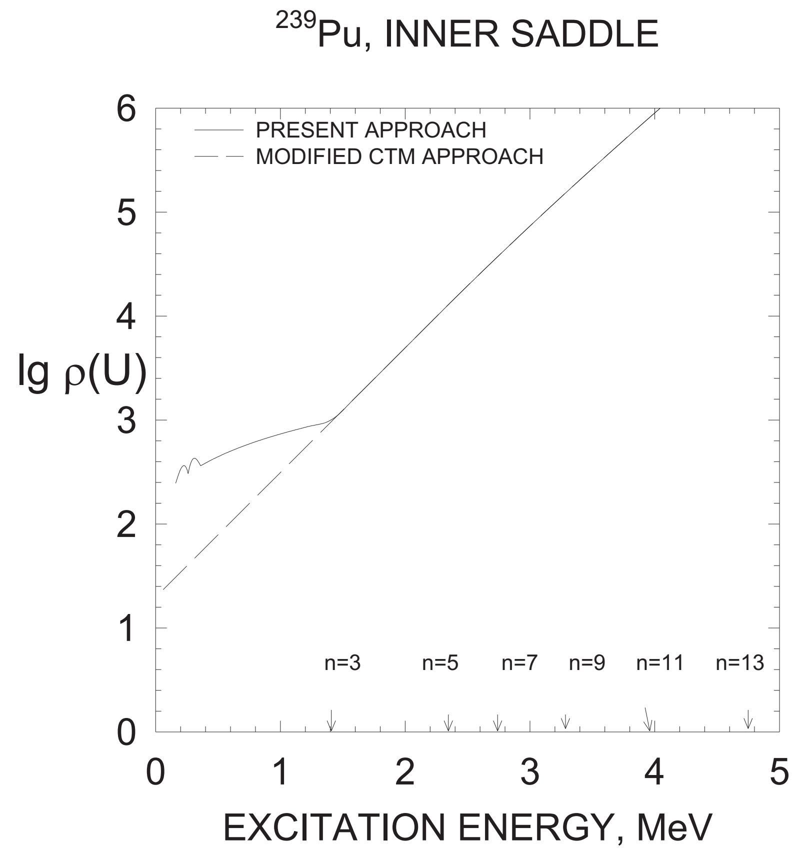

Figure 5.8: Level densities at inner saddle-point in ^{239}Pu. The arrows on the horizontal axis indicate excitation thresholds of odd $n-$quasi-particle configurations.

and Np nuclei were obtained essentially within the same approach [5.64–5.66]. In the latter case, however, the parameters should be treated as rather crude estimates, due to the more complex structure of fission barriers in Th and Pa as compared to the transuranium nuclei.

Fission barrier parameters: inner(A) and outer(B) barrier heights ($E_{fA(B)}$) and curvatures ($\hbar\omega_{A(B)}$) are given in Table 5.7. The symbol SYM denotes the symmetry of saddle point deformation. Comparison of the obtained results with the fission barriers determined by Smirenkin [5.67] shows the following: (i) for isotopes of uranium the agreement is rather good for outer fission barriers, while the isotopic dependencies for the inner barriers are similar, (ii) for Pu and Am the agreement is also good, except the americium outer barrier for neutron-deficient isotopes. It should be noted that the recommended barriers for neutron-deficient Am nuclei were determined from the analysis of the data for the ^{241}Am(n,f) reaction [5.59]. The largest discrepancies are observed in the case of outer barriers in Cm.

5.2.3 Conclusions and Recommendations

Recommended sophistication of the level density model, as compared to the conventional approaches, is needed in order to reproduce experimental data with the consistent level density and barrier parameters. It should be stressed, that the use of the recommended fission barriers also implies the use of the described approach to the level densities above the inner and outer saddle-points. The recommended fission barrier parameters are contained in **maslov.dat** file.

Table 5.7: Fission barrier parameters.

Nuclide	E_{fA},MeV	Sym.(A)	E_{fB},MeV	Sym.(B)	$\hbar\omega_A$,MeV	$\hbar\omega_B$,MeV	Δ_f,MeV
^{230}Th	6.1	S	6.8	MA	0.9	0.6	0.832
^{231}Th	6.0	S	6.7	MA	0.7	0.5	0.830
^{232}Th	5.8	S	6.7	MA	0.9	0.6	0.828
^{233}Th	5.1	S	6.65	MA	0.7	0.5	0.806
^{230}Pa	5.6	S	5.8	MA	0.6	0.4	0.802
^{231}Pa	5.5	S	5.5	MA	1.0	0.5	0.800
^{232}Pa	5.0	S	6.4	MA	0.6	0.4	0.828
^{233}Pa	5.7	S	5.8	MA	1.0	0.5	0.808
^{234}Pa	6.3	S	6.15	MA	0.6	0.4	0.806
^{231}U	4.4	S	5.5	MA	0.7	0.5	0.869
^{232}U	4.9	S	5.4	MA	0.9	0.6	0.848
^{233}U	4.35	S	5.55	MA	0.8	0.5	0.946
^{234}U	4.8	S	5.5	MA	0.9	0.6	0.889
^{235}U	5.25	S	6.0	MA	0.7	0.5	0.803
^{236}U	5.0	S	5.67	MA	0.9	0.6	0.833
^{237}U	6.4	GA	6.15	MA	0.7	0.5	0.809
^{238}U	6.3	GA	5.5	MA	1.0	0.6	0.818
^{239}U	6.45	GA	6.0	MA	0.7	0.5	0.816
^{236}Np	5.9	GA	5.4	MA	0.6	0.4	0.821
^{237}Np	6.0	GA	5.4	MA	1.0	0.5	0.819
^{238}Np	6.5	GA	5.75	MA	0.6	0.4	0.820
^{237}Pu	5.10	S	5.15	MA	0.7	0.5	0.799
^{238}Pu	5.6	S	5.1	MA	0.9	0.6	0.818
^{239}Pu	6.2	GA	5.7	MA	0.7	0.5	0.816
^{240}Pu	6.05	GA	5.15	MA	0.9	0.6	0.875
^{241}Pu	6.15	GA	5.50	MA	0.7	0.5	0.855
^{242}Pu	5.85	GA	5.05	MA	0.9	0.6	0.846
^{243}Pu	6.05	GA	5.45	MA	0.7	0.5	0.910
^{244}Pu	5.7	GA	4.85	MA	0.9	0.6	0.848
^{245}Pu	5.85	GA	5.25	MA	0.7	0.5	0.855
^{239}Am	6.00	GA	5.40	MA	0.8	0.5	0.776
^{240}Am	6.10	GA	6.00	MA	0.6	0.4	0.775
^{241}Am	6.00	GA	5.35	MA	0.8	0.5	0.773
^{242}Am	6.32	GA	5.78	MA	0.6	0.4	0.884
^{243}Am	6.40	GA	5.05	MA	1.0	0.5	0.770
^{244}Am	6.25	GA	5.9	MA	0.7	0.53	0.808
^{241}Cm	7.15	GA	5.5	MA	0.7	0.5	0.793
^{242}Cm	6.65	GA	5.0	MA	0.9	0.6	0.811
^{243}Cm	6.33	GA	5.4	MA	0.7	0.5	0.810
^{244}Cm	6.18	GA	5.10	MA	0.9	0.6	0.868
^{245}Cm	6.35	GA	5.45	MA	0.7	0.5	0.867
^{246}Cm	6.00	GA	4.80	MA	0.9	0.6	0.865
^{247}Cm	6.12	GA	5.10	MA	0.7	0.5	0.883
^{248}Cm	5.80	GA	4.80	MA	0.9	0.6	0.842
^{249}Cm	5.63	GA	4.95	MA	0.7	0.5	0.900

S - symmetric saddle point, GA - axially asymmetric saddle point, MA - mass asymmetric saddle point.

5.3 Partial Level Densities

Coordinator: M.B. Chadwick

Summary

Methods for calculating partial level densities for use in pre-equilibrium model calculations are described.

The RIPL Starter File includes a Fortran code **avrigeanu.for** by M. Avrigeanu for using various equidistant and Fermi-gas single-particle models, including models that incorporate pairing and shell effects within closed-form treatments and a Fortran code *capote_micro.for* by R. Capote, which uses a microscopic theory based on a convolution of shell-model single-particle states with BCS pairing.

5.3.1 Introduction

The partial level density (or "state density") is used in pre-equilibrium reaction calculations to describe the statistical properties of particle-hole excitations. Numerous theoretical methods have been developed to determine these partial level densities, and a variety of approaches have been used by researchers in pre-equilibrium calculations. Some of these approaches address theoretical methods for incorporating physical phenomena such as shell effects and pairing.

Despite the extensive amount of research that has been undertaken into the computation of partial level densities, even the most sophisticated theoretical predictions can significantly deviate from reality. There is a difficulty in testing the validity of calculated partial densities through comparisons between calculated and measured pre-equilibrium spectra because of uncertainties in our understanding of pre-equilibrium reaction mechanisms. A useful collection of articles on state-of-the-art methods for the calculation of partial level densities is the proceedings of the *Nuclear Level Densities* conference in Bologna [5.68].

One of the most widely used approaches is to determine partial level densities within an equidistant single-particle model, as proposed by Williams [5.69]. An important modification to limit the holes to excitation energies less than the nuclear well depth was made by Běták and Dobeš [5.70]. This is summarized below. A useful work which utilizes a computation of partial level densities from single-particle shell-model states within an applications-oriented Williams-type expression, is the work of M. Herman, G. Reffo *et al.* [5.71]. However, electronic files containing the numerical values determined in this work are unavailable.

5.3.2 Equidistant Formula with Well-Depth Restrictions

Since partial level densities based on equidistant levels are widely used in pre-equilibrium calculations because of their simplicity, we provide expressions for their determination below.

The density of p-particle h-hole states with residual nucleus energy U can be partitioned into the energy-dependent density multiplied by a spin distribution, $\rho(p,h,U,l) = \omega(p,h,U)\ R_n(l)$. The equidistant model expression for the energy dependent density with finite hole-depth restrictions is [5.70]

$$\omega(p,h,U) = \frac{g^n}{p!h!(n-1)!}\sum_{j=0}^{h}(-1)^j\binom{h}{j}(U-\Delta-A_{ph}-j\epsilon_F)^{n-1}$$
$$\times\ \Theta(U-\Delta-\alpha_{ph}-j\epsilon_F), \tag{5.47}$$

where $n = p+h$, g is the single particle density, ϵ_F is the Fermi energy, Δ is the pairing energy, and $A_{ph} = (p^2+h^2+p-3h)/4g$ accounts for Pauli blocking, and $\alpha_{ph} = (p^2+h^2)/2g$. The Θ-function is unity if its argument is positive, and zero otherwise. The single-particle density is often taken as $g = A/13$, which approximates the average single-particle density near the Fermi energy. Numerous possibilities for the pairing energy Δ have been suggested; a particularly useful approach is the "advanced pairing model" of Fu, which is mentioned below.

A Gaussian spin distribution is usually adopted,

$$R_n(l) = \frac{2l+1}{2\sqrt{2\pi}\sigma_n^3}\exp\left[-\frac{(l+1/2)^2}{2\sigma_n^2}\right], \tag{5.48}$$

where l is the spin and σ_n is the spin cut-off parameter, often taken as $\sigma_n^2 = 0.24nA^{2/3}$ [5.72].

The above expression is applicable in many pre-equilibrium model calculations. However, a useful extension of this formula to cases where the particle-excitations are also restricted, has been made by Obložinský [5.73]. This form is particularly useful in quantum mechanical multistep compound calculations where the particle excitations remain bound.

5.3.3 Analytical Formulae

The RIPL Starter File includes a code, **avrigeanu.for**, written by Avrigeanu *et al.* [5.74], to calculate partial level densities from a variety of models. The partial level density models computed by this code are described in detail in Avrigeanu *et al.*'s extensive report [5.74], and are summarized below:

1. The one-component Williams formula, which uses equidistant single-particle levels [5.69];
2. The two component (i.e. distinguishing neutron and proton excitations) Williams formula, which uses equidistant single-particle levels;
3. The one and two component formula versions of the Williams formula with finite well-depth restrictions, due to Běták and Dobeš [5.70];
4. The one and two component formula versions of the Williams formula with finite well-depth and binding-energy restrictions, due to Obložinský [5.73];
5. The advanced pairing correction formulae of Fu [5.55], using the one-component Fu model;
6. The Kalbach formula for one-component partial level densities with pairing considerations [5.75];
7. The Kalbach formula based on single-particle and hole levels with a Fermi-gas energy dependence [5.76]. The nuclear potential finite-depth correction factor for a one-component Fermi-gas is also determined [5.76];
8. The Mao formula, including Pauli-exclusion effects [5.77].

5.3.4 Microscopic Theory

Most semi-empirical approaches to calculating partial level densities are based on various simplifying approximations. In particular, such approaches often inadequately account for shell effects, pairing effects and parity distributions. To address these deficiencies, more involved microscopical methods have been developed to calculate more realistic particle-hole level densities using the single-particle level scheme of the shell model. Additionally, the BCS formalism has been included in order to account more properly for pairing effects. In the combinatorial method the level density is calculated numerically by performing an exhaustive counting of the nuclear excited configurations.

The other file *capote_micro.for* is a Fortran code, included in the RIPL Starter File by R. Capote and R. Pedrosa [5.78]. It allows for microscopic calculations of particle-hole partial level densities (up to $3p-3h$ for even-even nuclei), which represent the dominant contribution to the pre-equilibrium component of emission spectra. Shell-model single-particle levels are taken from the Möller-Nix compilation [5.40].

The *capote_micro.for* code is a more recent (and rewritten) version of Herman and Reffo's ICAR code described in Ref. [5.79].

5.3.5 Conclusions and Recommendations

For detailed studies of the role of partial level densities in pre-equilibrium calculations, microscopic calculations using the *capote_micro.for* code may be performed. Such calculations include shell, and pairing effects. However, the results of such calculations should always be treated with caution, as the predictive capability of all partial level density theories is limited. For many pre-equilibrium calculations, particularly for applications, the more phenomenological models included in Avrigeanu's **avrigeanu.for** code are useful. Again, though, the limitations of such partial level density predictions should be kept in mind.

References

[5.1] H. Bethe, Rev. Mod. Phys. **9**, 69 (1937).

[5.2] A.V. Ignatyuk, M.G. Itkis, V.N. Okolovich, G.N. Smirenkin and A.S. Tishin, J. Sov. Nucl. Phys. **21**, 612 (1975).

[5.3] S.K. Kataria and V.S. Ramamurthy, Nucl. Phys. **A349**, 10 (1980).

[5.4] W. Reisdorf, Z. Phys. **A300**, 227 (1981).

[5.5] J. Toke and W.J. Swiatecki, Nucl. Phys. **A372**, 141, (1981).

[5.6] J.M. Lang and K.J. Le Couteur, Proc. Phys. Soc. **A67**, 586 (1954).

[5.7] E. Erba, U. Facchini and E. Saetta-Menichella, Nuovo Cim. **22**, 1237 (1961).

[5.8] A. Gilbert and A.G.W. Cameron, Can. J. Phys. **43**, 1446 (1965).

[5.9] J.E. Lynn, *Theory of Neutron Resonance Reactions* (Clarendon Press, Oxford 1968).

[5.10] A.V. Malyshev, *Level Density and Structure of Atomic Nuclei* (in Russian). (Atomizdat, Moscow 1969).

[5.11] H. Baba, Nucl. Phys. **A159**, 625 (1970).

[5.12] W. Dilg, W. Schantl, H. Vonach and M. Uhl, Nucl. Phys. **A217**, 269 (1973).

[5.13] S.K. Kataria, V.S. Ramamurthy and S.S. Kapoor, Phys. Rev. **C18**, 549 (1978).

[5.14] G. Reffo, *in* Nuclear Theory for Applications. IAEA-SMR-43, Trieste, 1980, p. 205.

[5.15] A.S. Iljinov, M.V. Mebel *et al.*, Nucl. Phys. **A543**, 517 (1992).

[5.16] T. Ericson, Adv. Phys. **9**, 425 (1960).

[5.17] J.L. Cook, H. Ferguson and L. Musgrov, Aust. J. Phys. **20**, 477 (1967).

[5.18] Su Zongdi, Zhuang Youxiang, Wang Cuilan, Zhou Chunmei, Report INDC(CPR)-2 (IAEA Vienna 1985).

[5.19] A.V. Ignatyuk, V.S. Stavisski and Yu.N. Shubin, *in* Nuclear Data for Reactors. IAEA Vienna, 1970.

[5.20] V.S. Ramamurthy, S.S. Kapoor and S.K. Kataria, Phys. Rev. Lett. **25**, 386 (1970).

[5.21] S. Goriely, Nucl. Phys. **A605**, 28 (1996).

[5.22] A.V. Ignatyuk, G.N. Smirenkin and A.S. Tishin, J. Sov. Nucl. Phys. **21**, 255 (1975).

[5.23] W.D. Myers and W.J. Swiatecki, Ark. Fysik **36**, 593 (1967).

[5.24] A. Mengoni and Y. Nakajima, J. Nucl. Sci. Tech. **31**, 151 (1994).

[5.25] Huang Zhongfu, He Ping, Su Zongdi and Zhou Chunmei, Chin. J. Nucl. Phys., **13**, 147 (1991).

[5.26] T. Belgya, G. Molnár, B. Fazekas and J. Östör, Report INDC(NDS)-367 (IAEA Vienna 1997).

[5.27] A.V. Ignatyuk, *Statistical Properties of Excited Atomic Nuclei* (in Russian). (Energoatomizdat, Moscow 1983); Translated by IAEA, Report INDC-233(L) (IAEA Vienna 1985).

[5.28] A.V. Ignatyuk, K.K. Istekov and G.N. Smirenkin, Sov. J. Nucl. Phys. **29**, 450 (1979).

[5.29] A.V. Ignatyuk, J.L. Weil, S. Raman and S. Kahane, Phys. Rev. **C47**, 1504 (1993).

[5.30] A. Bohr, B. Mottelson, *Nuclear Structure, vol 2* (Benjamin Inc., New York and Amsterdam, 1974).

[5.31] G. Hansen and A. Jensen, Nucl. Phys. **A406**, 236 (1983).

[5.32] G. Maino, A. Mengoni and A. Ventura, Phys. Rev. **C42**, 988 (1990).

[5.33] E.M. Rastopchin, M.N. Svirin and G.N. Smirenkin, Sov. J. Nucl. Phys. **52**, 1258 (1990).

[5.34] A.V. Ignatyuk, *in* Nuclear Data Evaluation Methodology, Ed. Ch. Dunford (World Scientific, Singapore 1992), p. 411.

[5.35] O.T. Grudzevich, A.V. Ignatyuk, V.I. Plyaskin and A.V. Zelenetsky, *in* Nuclear Data for Science and Technology (Mito, 1988), JAERI, p. 187.

[5.36] W.D. Myers, Droplet Model of Atomic Nuclei. Plenum Press, 1977.

[5.37] A.V. Ignatyuk, Contribution to the 3rd CRP Meeting on RIPL, Trieste, 1997.

[5.38] Lu Guoxiong, Dong Liaoyuan, Huang Zhongfu, Qiu Guochun, Su Zongdi, Contribution to the 3-rd CRP Meeting on RIPL, Trieste, 1997.

[5.39] A.V. Ignatyuk, K.K. Istekov, V.N. Okolovich and G.N. Smirenkin G.N, *in* Physics and Chemistry of Fission, IAEA, Vienna, 1980, v. 1, p. 21.

[5.40] P. Möller, J.R. Nix, W.D. Myers and W.J. Swiatecki, Atomic Data Nucl. Data Tbl. **59**, 185 (1995).

[5.41] J.R. Nix, Private communication to M. Herman, 1988.

[5.42] V.M. Strutinsky, Nucl. Phys. **A95**, 420 (1967).

[5.43] W.M. Howard and P. Möller, Atomic Data Nucl. Data Tbl. **25**, 219 (1980).

[5.44] T. Dossing, T.I. Khoo, T. Lauritsen *et al.*, Phys. Rev. Lett. **75**, 1276 (1995).

[5.45] S.T. Boneva, V.A. Khitrov, Yu.V. Popov and A.M. Sukhovoj, *in* Proc. IV International Seminar on Interaction of Neutrons with Nuclei, Dubna, Russia, April 27-30, 1996, Report E3-96336 (JINR Dubna 1996), p. 183.

[5.46] V.M. Maslov, *in* Proc. IV International Seminar on Interaction of Neutrons with Nuclei, Dubna, Russia, April 27-30, 1996, Report E3-96336 (JINR Dubna 1996), p. 326.

[5.47] A.V. Ignatyuk and V.M. Maslov, Sov. J. Nucl. Phys. **54**, 392 (1991).

[5.48] A.V. Ignatyuk and V.M. Maslov, *in* Proc. Int. Symp. Nuclear Data Evaluation Methodology, Brookhaven,USA, October 12-16, 1992 (World Scientific, Singapore 1993), p. 440.

[5.49] V.M. Maslov and Y. Kikuchi, JAERI-Research 96-030, 1996.

[5.50] S. Bjornholm and J.E. Lynn, Rev. Mod. Phys. **52**, 725 (1980).

[5.51] Yu.V. Porodzinskij, E.Sh. Sukhovitskij and V.M. Maslov *in* Int. Conf. Nucl. Data Sci. and Technology, Trieste, Italy, May 19-23, 1997.

[5.52] V.M. Maslov, Z. Phys. **A347**, 211 (1994).

[5.53] V.M. Maslov, *in* Proc. 9th Int. Symp. Capture Gamma-Ray Spectroscopy and Related Topics, Budapest, Hungary, October 8-12, 1996, to be published.

[5.54] V.M. Maslov, *in* Int. Conf. Nucl. Data for Sci. and Technology, Trieste, Italy, May 19-23, 1997.

[5.55] C.Y. Fu, Nucl. Sci. Eng. **86**, 344 (1984); C.Y. Fu, Nucl. Sci. Eng. **92**, 440 (1986).

[5.56] M. Bolsterli, E.O. Fiset, J.R. Nix and J.L. Norton, Phys. Rev. **C5**, 1050 (1972).

[5.57] P.C. Sood and R.N. Singh, Nucl. Phys. **A373**, 519 (1982).

[5.58] V.M. Maslov *et al.*, Report INDC(BLR)-4 (IAEA Vienna 1996).

[5.59] V.M. Maslov *et al.*, Report INDC(BLR)-5 (IAEA Vienna 1996).

[5.60] V.M. Maslov and Y. Kikuchi, Nucl. Sci. Eng. **124**, 492 (1996).

[5.61] V.M. Maslov *et al.*, Report INDC(BLR)-7 (IAEA Vienna 1997).

[5.62] V.M. Maslov *et al.*, Report INDC(BLR)-9 (IAEA Vienna 1997).

[5.63] V.M. Maslov, submitted for publication to Sov. J. Nucl. Phys., 1997.

[5.64] V.M. Maslov, Ann. Nucl. Energy **19**, 181 (1992).

[5.65] V.M. Maslov, Yadernye Konstanty **1**, 80 (1992).

[5.66] V.M. Maslov, Yadernye Konstanty **4**, 19 (1987).

[5.67] G.N. Smirenkin, Report INDC(CCP)-359 (IAEA Vienna 1993).

[5.68] Proceedings of the Nov 15-17, 1989 conference in Bologna, *Nuclear Level Densities*, Ed. G. Reffo, M. Herman, and G. Maino (World Scientific, Singapore 1992).

[5.69] F.C. Williams, Nucl. Phys. **A166**, 231 (1971).

[5.70] E. Běták and J. Dobeš, Z. Phys. **A279**, 319 (1976).

[5.71] M. Herman, G. Reffo, *et al.*, Phys. Rev. **C40**, 2870 (1989).

[5.72] H. Gruppelaar, *in IAEA Advisory Group Meeting on Basic and Applied Problems on Nuclear Level Densities.* Ed. M.R. Bhat (Brookhaven National Laboratory 1983), p. 143.

[5.73] P. Obložinský, Nucl. Phys. **A453**, 127 (1986).

[5.74] M. Avrigeanu, A. Harangozo and V. Avrigeanu, "Development of Data Files with Partial Level Densities for Nuclear Data Calculations", IAEA Report (to be published); M. Avrigeanu, IAEA Research Contract No. 8886/RO/RBF.

[5.75] C. Kalbach, Nucl. Sci. Eng. **95**, 70 (1987); C. Kalbach, Z. Phys. **A332**, 157 (1989).

[5.76] C. Kalbach, Phys. Rev. **C32**, 1157 (1985).

[5.77] Mao Ming De and Guo Hua, J. Phys. **G19**, 421 (1993).

[5.78] R. Capote and R. Pedrosa, DENSIDAD code (1996), unpublished; Private communication to P. Obložinský of the IAEA (1997).

[5.79] M. Herman and G. Reffo, Phys. Rev. **C36**, 1546 (1987); M. Herman, G. Reffo and R.A. Rego, Phys. Rev. **C37**, 797 (1988).